

**AFRL-ML-WP-TR-2003-4022**

**NONDESTRUCTIVE EVALUATION  
(NDE) TECHNOLOGY INITIATIVES**

**Delivery Order 0021: Application of an  
Electrochemical Fatigue Sensor (EFS) Borescope  
System for Military Turbine Engine Assessment**



**R. Krupa  
R. Tillinghast  
T. Root**

**Materials Technologies, Inc.  
DBA Tensiodyne Scientific Corporation  
1161 San Vicente Blvd, Suite 707  
Los Angeles, CA 90049**

**Optim Incorporated  
64 Technology Park Road  
Sturbridge, MA 01566-1262**

**OCTOBER 2002**

**Final Report for 01 November 2000 – 31 October 2002**

**Approved for public release; distribution is unlimited.**

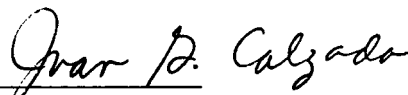
**MATERIALS AND MANUFACTURING DIRECTORATE  
AIR FORCE RESEARCH LABORATORY  
AIR FORCE MATERIEL COMMAND  
WRIGHT-PATTERSON AIR FORCE BASE, OH 45433-7750**

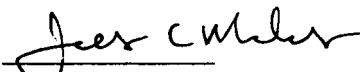
## NOTICE


WHEN GOVERNMENT DRAWINGS, SPECIFICATIONS, OR OTHER DATA ARE USED FOR ANY PURPOSE OTHER THAN IN CONNECTION WITH A DEFINITELY GOVERNMENT-RELATED PROCUREMENT, THE UNITED STATES GOVERNMENT INCURS NO RESPONSIBILITY OR ANY OBLIGATION WHATSOEVER. THE FACT THAT THE GOVERNMENT MAY HAVE FORMULATED OR IN ANY WAY SUPPLIED THE SAID DRAWINGS, SPECIFICATIONS, OR OTHER DATA, IS NOT TO BE REGARDED BY IMPLICATION OR OTHERWISE IN ANY MANNER CONSTRUED, AS LICENSING THE HOLDER OR ANY OTHER PERSON OR CORPORATION, OR AS CONVEYING ANY RIGHTS OR PERMISSION TO MANUFACTURE, USE, OR SELL ANY PATENTED INVENTION THAT MAY IN ANY WAY BE RELATED THERETO.

THIS REPORT IS RELEASABLE TO THE NATIONAL TECHNICAL INFORMATION SERVICE (NTIS). AT NTIS, IT WILL BE AVAILABLE TO THE GENERAL PUBLIC, INCLUDING FOREIGN NATIONS.

THIS TECHNICAL REPORT HAS BEEN REVIEWED AND IS APPROVED FOR PUBLICATION.

  
JUAN G. CALZADA, Project Engineer  
Nondestructive Evaluations Branch  
Metals, Ceramics & NDE Division

  
JAMES C. MALAS, Chief  
Nondestructive Evaluations Branch  
Metals, Ceramics & NDE Division

  
GERALD J. PETRAK, Assistant Chief  
Metals, Ceramics & NDE Division  
Materials & Manufacturing Directorate

IF YOUR ADDRESS HAS CHANGED, IF YOU WISH TO BE REMOVED FROM OUR MAILING LIST, OR IF THE ADDRESSEE IS NO LONGER EMPLOYED BY YOUR ORGANIZATION, PLEASE NOTIFY, AFRL/MLLP, WRIGHT-PATTERSON AFB OH 45433-7750 AT (937) 255-9819 TO HELP US MAINTAIN A CURRENT MAILING LIST.

COPIES OF THIS REPORT SHOULD NOT BE RETURNED UNLESS RETURN IS REQUIRED BY SECURITY CONSIDERATIONS, CONTRACTUAL OBLIGATIONS, OR NOTICE ON A SPECIFIC DOCUMENT.

| <b>REPORT DOCUMENTATION PAGE</b>  |                                    |                                     |   | <i>Form Approved</i><br><i>OMB No. 0704-0188</i>                                    |   |
|---|------------------------------------|-------------------------------------|---|---|---|
| The public reporting burden for this collection of information is estimated to average 1 hour per response, including the time for reviewing instructions, searching existing data sources, gathering and maintaining the data needed, and completing and reviewing the collection of information. Send comments regarding this burden estimate or any other aspect of this collection of information, including suggestions for reducing this burden, to Department of Defense, Washington Headquarters Services, Directorate for Information Operations and Reports (0704-0188), 1215 Jefferson Davis Highway, Suite 1204, Arlington, VA 22202-4302. Respondents should be aware that notwithstanding any other provision of law, no person shall be subject to any penalty for failing to comply with a collection of information if it does not display a currently valid OMB control number. <b>PLEASE DO NOT RETURN YOUR FORM TO THE ABOVE ADDRESS.</b>   |                                    |                                     |   |   |   |
| <b>1. REPORT DATE (DD-MM-YY)</b><br>October 2002  |                                    | <b>2. REPORT TYPE</b><br>Final      |   | <b>3. DATES COVERED (From - To)</b><br>11/01/2000 – 10/31/2002                      |   |
| <b>4. TITLE AND SUBTITLE</b><br>NONDESTRUCTIVE EVALUATION (NDE) TECHNOLOGY INITIATIVES<br>Delivery Order 0021: Application of an Electrochemical Fatigue Sensor (EFS)<br>Borescope System for Military Turbine Engine Assessment  |                                    |                                     |   | <b>5a. CONTRACT NUMBER</b><br>F33615-97-D-5271                                      |   |
|   |                                    |                                     |   | <b>5b. GRANT NUMBER</b>   |   |
|   |                                    |                                     |   | <b>5c. PROGRAM ELEMENT NUMBER</b><br>62102F   |   |
| <b>6. AUTHOR(S)</b><br>R. Krupa<br>R. Tillinghast<br>T. Root  |                                    |                                     |   | <b>5d. PROJECT NUMBER</b><br>4349   |   |
|   |                                    |                                     |   | <b>5e. TASK NUMBER</b><br>40  |   |
|   |                                    |                                     |   | <b>5f. WORK UNIT NUMBER</b><br>01   |   |
| <b>7. PERFORMING ORGANIZATION NAME(S) AND ADDRESS(ES)</b><br><div style="display: flex; justify-content: space-between;"> <div style="width: 45%;">           Materials Technologies, Inc.<br/>           DBA Tensiodyne Scientific Corporation<br/>           1161 San Vicente Blvd, Suite 707<br/>           Los Angeles, CA 90049         </div> <div style="width: 45%;">           Optim Incorporated<br/>           64 Technology Park Road<br/>           Sturbridge, Ma 01566-1262         </div> </div>  |                                    |                                     |   | <b>8. PERFORMING ORGANIZATION REPORT NUMBER</b><br>ES0408                           |   |
| <b>9. SPONSORING/MONITORING AGENCY NAME(S) AND ADDRESS(ES)</b><br>Materials and Manufacturing Directorate<br>Air Force Research Laboratory<br>Air Force Materiel Command<br>Wright-Patterson AFB, OH 45433-7750   |                                    |                                     |   | <b>10. SPONSORING/MONITORING AGENCY ACRONYM(S)</b><br>AFRL/MLLP                     |   |
| <b>12. DISTRIBUTION/AVAILABILITY STATEMENT</b><br>Approved for public release; distribution is unlimited.   |                                    |                                     |   | <b>11. SPONSORING/MONITORING AGENCY REPORT NUMBER(S)</b><br>AFRL-ML-WP-TR-2003-4022 |   |
|   |                                    |                                     |   |   |   |
| <b>13. SUPPLEMENTARY NOTES</b><br>Report contains color.  |                                    |                                     |   |   |   |
| <b>14. ABSTRACT</b><br><p>The objective for this project was to improve the United States Air Force's capability to perform fatigue assessment of military aircraft engines through the application of four nondestructive technologies: eddy current inspection, ultrasonic inspection, visual inspection, and the electrochemical fatigue sensor (EFS).</p> <p>EFS is a relatively new technology; the other three inspection methodologies are well established and widely accepted means of component inspection. A 6-mm-diameter inspection borescope, capable of delivering ultrasonic, eddy current, and EFS probes, along with video imaging, to fatigue critical locations within an engine has been developed. The 3-mm ID working channel within the borescope permits the delivery of the three probes. An intuitive user interface employing a mechanical joystick is used to articulate the borescope in all directions over a hemisphere of operation.</p> <p>While the EFS probe could be delivered, along with the electrolyte gel, through the borescope, the technology is not currently available to stress the turbine blades with enough force and control to permit EFS signal generation within the confines of an engine. Work is necessary in producing the loading mechanism within an engine, and on improving engine access on future designs.</p> |                                    |                                     |   |   |   |
| <b>15. SUBJECT TERMS</b><br>Electrochemical fatigue sensor, turbine engine, fiberscope, borescope, eddy current, ultrasonic   |                                    |                                     |   |   |   |
| <b>16. SECURITY CLASSIFICATION OF:</b>  |                                    |                                     | <b>17. LIMITATION OF ABSTRACT:</b><br>SAR | <b>18. NUMBER OF PAGES</b><br>38  | <b>19a. NAME OF RESPONSIBLE PERSON</b> (Monitor)<br>Juan G. Calzada<br><b>19b. TELEPHONE NUMBER</b> (Include Area Code)<br>(937) 255-1605 |
| <b>a. REPORT</b><br>Unclassified  | <b>b. ABSTRACT</b><br>Unclassified | <b>c. THIS PAGE</b><br>Unclassified |   |   |   |

# TABLE OF CONTENTS

| Section  | Page |
|--|------|
| Summary .....  | 1    |
| 1.0 Project Objectives.....                            | 2    |
| 2.0 Electrochemical Fatigue Sensor System.....         | 3    |
| 2.1 EFS Electrolyte Gel.....                           | 3    |
| 2.2 Load Generation .....                              | 5    |
| 2.3 EFS Data Collection.....                           | 7    |
| 2.4 EFS Signal .....                                   | 10   |
| 3.0 Ultrasonic Inspection.....                         | 13   |
| 4.0 Eddy Current Inspection.....                       | 15   |
| 5.0 Borescope Delivery System.....                     | 16   |
| 6.0 Conclusions .....                                  | 22   |
| Appendix A. Borescope Detail Drawings List .....       | 23   |
| Appendix B. EFS Electronics Settings .....             | 26   |
| Appendix C. Eddy Current Probe Standard Programs ..... | 28   |
| Appendix D. Ultrasonic Probes Standard Programs .....  | 29   |

## LIST OF FIGURES

| Figure  | Page |
|---|------|
| 1. EFS Probe.....   | 4    |
| 2. Schematic Representation of Load Actuator and Test Sample..... | 5    |
| 3. Photograph of Actuator and Sample .....                        | 6    |
| 4. EFS Bench Top Block Diagram.....                               | 9    |
| 5. Potentiostat Output.....                                       | 10   |
| 6. EFS Noise .....  | 11   |
| 7. 5Hz and 10Hz Filtered EFS Signals.....                         | 12   |
| 8. Ultrasound Probes.....   | 13   |
| 9. Delay Line Ultrasonic Display of 0.080" Thick Test Plate.....  | 13   |
| 10. Surface Wave Ultrasonic Signal of Distant Crack.....          | 14   |
| 11. Absolute Eddy Current Signals from 0.005" Wide Cracks.....    | 15   |
| 12. Articulation Link Pair .....                                  | 18   |
| 13. Borescope Assembly .....                                      | 20   |

## SUMMARY

The objective for this project was to improve the United States Air Force's capability to perform fatigue assessment of military aircraft engines through the application of four nondestructive technologies: eddy current inspection, ultrasonic inspection, visual inspection, and the electrochemical fatigue sensor.

While the electrochemical fatigue sensor (EFS) is a relatively new technology, the other three inspection methodologies are well established and widely accepted means of component inspection. A 6mm diameter inspection borescope, capable of delivering ultrasonic, eddy current, and EFS probes, along with video imaging, to fatigue critical locations within an engine has been developed. The 3mm ID working channel within the borescope permits the delivery of the three probes. An intuitive user interface employing a mechanical joystick is used to articulate the borescope in all directions over a hemisphere of operation.

While the EFS probe could be delivered, along with the electrolyte gel, through the borescope, the technology is not currently available to stress the turbine blades with enough force and control to permit EFS signal generation within the confines of an engine. Work is necessary in producing the loading mechanism within an engine, and on improving engine access on future designs.

## 1.0 Project Objectives

The overall objective for this project is to improve the United States Air Force's capability to perform fatigue assessment of military aircraft engines through the application of four nondestructive technologies:

- ❑ Eddy Current Inspection
- ❑ Ultrasonic Inspection
- ❑ Visual Inspection Through a Flexible Borescope
- ❑ Electrochemical Fatigue Sensor

While the electrochemical fatigue sensor (EFS) is a relatively new technology, the other three inspection methodologies are well established and widely accepted means of component inspection. However, this is the first instrument that permits the delivery of eddy current (EC) and ultrasonic (UT) transducers, under visual guidance, to the internal components of an aircraft engine through standard borescope access ports in the engine's housing. The EFS sensor is also capable of being delivered to fatigue critical locations within an engine. However, technological advances in force generators are not currently capable of producing the load required to generate EFS signals within the tight space constraints of today's aircraft engines.

## 2.0 Electrochemical Fatigue Sensor System

A bench top load generation system was developed in order to evaluate the mechanism required to produce an EFS signal, and to verify that the data collection scheme produced the required signal-to-noise ratio necessary for measuring an EFS signal.

### 2.1 EFS Electrolyte Gel

The electrolyte gel used for this work was prepared by making a concentrated solution of the water-soluble salts that is later added to a gel forming suspension. For the preparation of 1L of the electrolyte gel, the following procedure was employed:

1. Weigh out 16.6g Boric Acid (CAS#10043-35-3), 28.6g Hydrated Sodium Borate (CAS#1303-96-4), and 1.5g Hydrated Sodium Molybdate (CAS#10102-40-6).
2. Dissolve the above salts in 200mL deionized water brought to a temperature of approximately 60°C using a double boiler. At room temperature, the salts do not readily dissolve completely at this concentration.
3. Weigh out 18.75g Laponite RD and 18.75g Laponite RDS (Southern Clay Products, Inc., 1212 Church St., Gonzales, TX 78629, 830-672-2891).
4. In a 1500mL glass beaker, add 800mL of deionized water. Stir the water with a propeller blade at 600-700 RPM. To the stirred water, slowly add the Laponite powders at a rate of approximately 1g/minute, taking care not to add more than 200mg at a time to the water mixture. If more than this is added at once, the clay powder will form clumps and will not properly disperse in the liquid. After all the Laponite powder is added to the beaker, continue stirring the suspension for approximately 30 additional minutes.
5. Add the 200mL of electrolyte concentrate to the stirred clay suspension slowly over a period of approximately 5 minutes. After all the electrolyte solution has been added, continue stirring for an additional 30 minutes.
6. Immediately after this 30-minute stirring period, pour the mixture into a 1L Nalgene bottle and tightly secure the top of the bottle. The mixture is thixotropic, and will become gelatinous in a few minutes.
7. To use the gel, shake the Nalgene bottle vigorously for 60 seconds. This will reduce the viscosity of the gel to the point where it can be poured. Upon storage of the gel, a small volume of water will accumulate on the surface of the gel material. Be sure to mix the mixture prior to taking a portion of the gel from the container in order to maintain the proper concentration of the aliquot taken, and the remaining gel.

For delivery of the gel through the borescope, a 15cc syringe is used to sample a portion of the recently mixed gel. The gel can be pushed down a length of 2mm OD tubing to the distal end of the borescope within a few minutes of loading the syringe. Once the gel has left the tubing (onto the sample), its viscosity will increase rapidly. If the gel is not used within a few minutes of loading the syringe, shake the syringe to mix the gel until a significant decrease in viscosity is observed (approximately 30-60 seconds). The gel is spread over the area that is to be interrogated by the EFS



electronics. Large areas, greater than one square inch, can be interrogated in a single EFS measurement. However, while spreading the gel over a large area increases the speed of analysis, it sacrifices spatial resolution. An EFS signal indicative of a crack cannot be pinpointed more accurately than the area of the area covered by the electrolyte gel.

At the proximal end of the tubing is a box containing a “T” tube with one side arm connected to the gel delivery syringe, and the other connected to a BNC connector mounted on the side of the box. Running the length of the 2mm tubing, and exiting the tube in a “T” connection, is a shielded copper wire attached to a small section of 2mm OD stainless steel tubing at the distal end of the probe. Over the stainless steel tubing, and overlapping the 2mm tubing slightly, is a small piece of heat shrink material. The heat shrink extends slightly beyond the stainless electrode so that the tip of the probe can be in direct contact with the gel, and even the grounded sample, without the electrode making direct contact with the sample. Once the tip of the probe is placed into the recently deposited gel, the stainless tubing acts as the EFS electrode.

The EFS electrode is constructed of a 10mm x 2mm OD stainless steel tube soldered to the shielded cable running the length of the 2mm OD PEBAX tubing. Stainless steel by itself produces a very poor electrode for the conduction of the small electrochemical current produced. Therefore, the stainless steel surface is electroplated with catalytic platinum black. This is done by immersing the steel in a solution of approximately 3.5% Chloroplatinic Acid (CAS# 16941-12-1) and 0.5% Lead Acetate (CAS# 6080-56-4), and applying a current density of approximately 30mA/cm<sup>2</sup> through the solution. This was accomplished by connecting a 9V battery to the stainless steel tubing (+) and a platinum wire (-) through a 477Ω current limiting resistor. Current was allowed to flow for a period of approximately 5 minutes, after which time the stainless tubing was rinsed in deionized water. The appearance of the stainless at this point is a dull black due to the high surface area of the platinum coating.

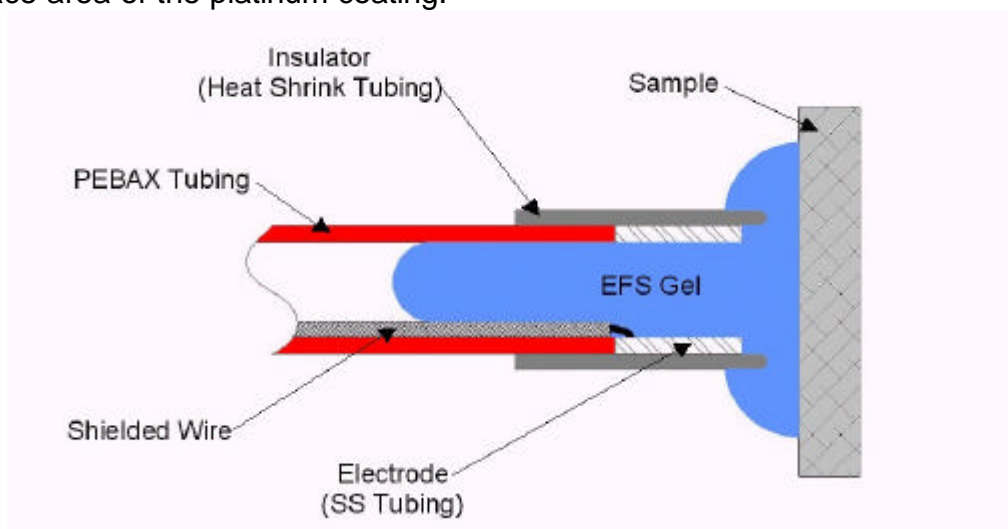


Figure 1. EFS Probe

## 2.2 Load Generation

The bench top load generator system consisted of a means to hold a test sample, and a mount for the load generator. A BEI KIMCO Linear Actuator, Model #LA24-200-000A, was driven with the sinusoidal output current from a KEPCO Op Amp, Model #BOP-20-10M. The sine wave reference signal was generated by a lock-in amplifier, and was amplified by the op-amp to produce the desired output force at the linear actuator. For the bench top actuator, the sinusoidal force on the sample had a minimum of 4 pounds and a maximum of 15 pounds; or an 11-pound AC force with a 9.5-pound DC component. This corresponded to an 18ksi sinusoidal load on the sample, with a DC offset of 16ksi. The offset ensured that the test piece was always under a load so that the linear actuator remained in contact with the sample at all times. This resulted in a pure sinusoidal load applied to the test sample. If the actuator were permitted to retract completely from the test sample, the sinusoidal wave pressure would be interrupted, and the resulting signal would be a complex function rather than a simple sine wave. The load generator action on the sample is schematically shown in Figure 2.

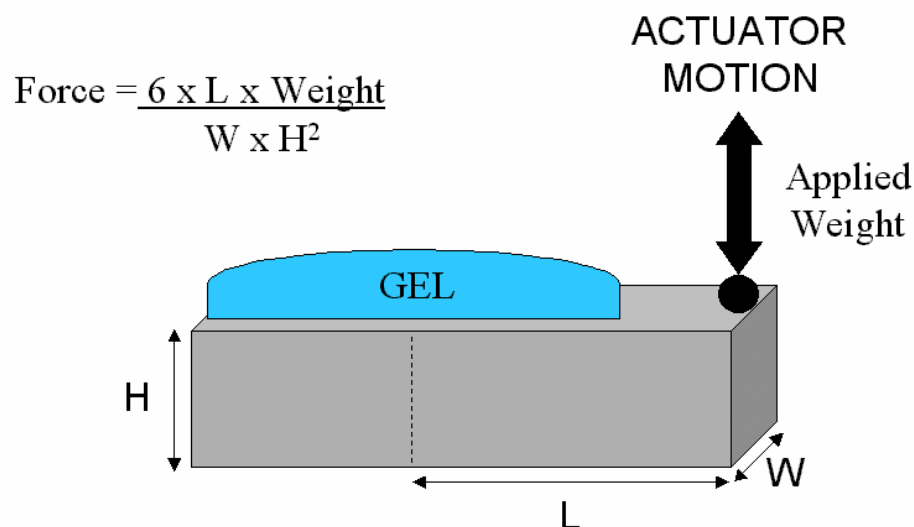


Figure 2. Schematic Representation of Load Actuator on Test Sample.

With this system, we were capable of producing up to 40ksi load on the sample, which compared favorably with previous studies in which EFS signals were generated with 10-30ksi. Figure 3 is a photograph of the system in operation.

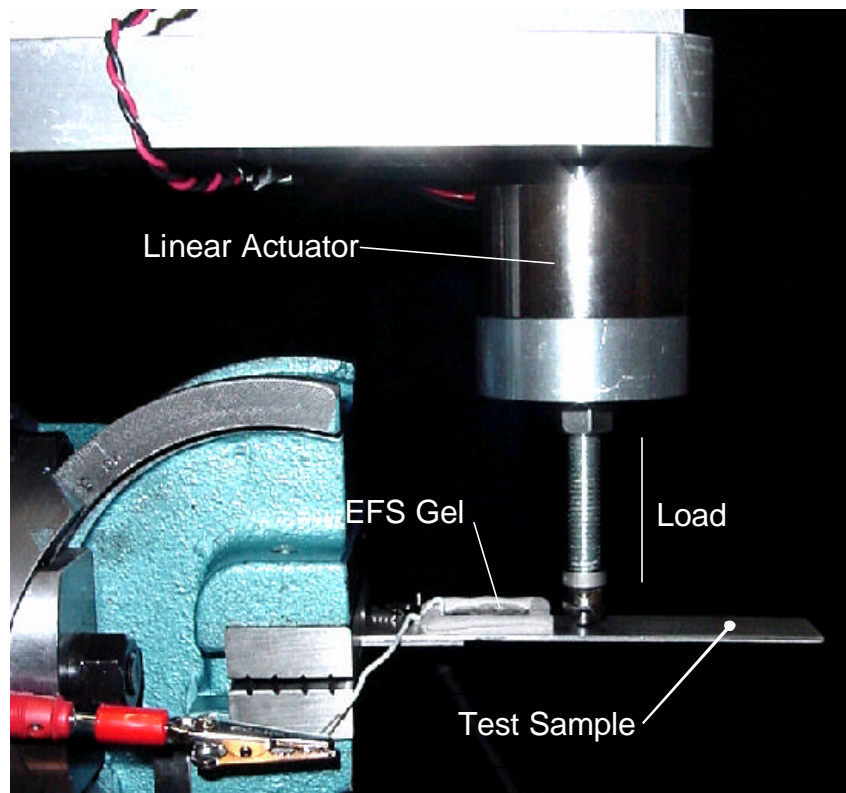


Figure 3. Photograph of Actuator and Sample.

While the application of the load required to produce an EFS signal on the bench top sample was accomplished with readily available components, generating a load of 10 pounds or more within the confines of an engine was more challenging.

In order to produce the desired EFS signal, a force of 8-10 pounds is required to produce 0.1% strain at the turbine blade root, assuming the load is applied to the tip of the blade. This requires the displacement at the blade tip reach 0.5-1mm. In other words, the actuator must have a 0.5-1mm displacement capability. In addition to the sinusoidal displacement required, a static displacement of 1-4mm is required because of the movement of the blade within the engine when it is at ambient temperature (thermal expansion holds the blade firmly in place when the engine is in operation and at an elevated temperature). The additional requirements for the actuator are it must fit through a 6.3mm diameter borescope access hole in the engine, and it must operate at a frequency above 1Hz, preferably above 5Hz. We investigated several different actuators for this application.

A stack of piezoelectric transducers (PZT) can generate forces up to approximately 200 pounds, and at frequencies up to approximately 5KHz. These ceramic materials can be quite small in diameter, on the order of 5-6mm, but the displacement for each individual transducer is only a fraction of what is required to produce the displacement required for this application. Even a stack of transducers on the order of 2" long would only produce

a displacement of a few thousands of an inch. This is much less than is required for the current application.

Electronic solenoids are capable of the required displacement, and capable of an offset displacement able to rigidly hold the blade in place during the measurement. The frequency response of this type of actuator is adequate for the application, with frequency responses in the tens of Hz quite common. However, under 10mm in diameter, electronics solenoids do not have the force generating capability necessary to generate the required 8-10 pounds of force on the blade.

There are a variety of ultrasonic motion devices, loosely classified as ultrasonic motors that are capable of meeting the displacement and force requirements for this application. However, the size of this class of devices is quite large (>10mm).

Magnetorestrictive material, such as terfenol, suffers from its inability to produce the required displacement, with most materials having motion ranges in the sub-millimeter range. It is also unclear at present if material is available in a small package size that is capable of generating the force required.

Liquid pressure in the form of a piston has the potential to generate the required force and displacement. However, the frequency response is quite low, and the size above the necessary 6mm maximum.

Lastly, we investigated the original concept of wedging a washer between the blade tip and its seal. The use of an engine turning tool could then be utilized to rotate the engine against the resistance of this wedge, producing the required force at the blade root. This approach could quite possibly generate the force required for EFS signal generation, but would be time consuming in its implementation in actual usage (requiring the insertion and retraction of two borescopes and washer for each blade to be interrogated). Additionally, the engine turning tool and engine transmissions we investigated had a very large amount of radial play, as much as several degrees, and a large amount of backlash. Because of the play between the input device (engine turning tool motor) and the resulting force on the individual turbine blade, the irreproducibility of the resultant force would undoubtedly be the limiting noise component in the system.

## 2.3 EFS Data Collection

In our experimentation, the part under interrogation was at ground potential, and a wire placed into the EFS gel, but not in contact with the sample, was connected to the Counter and Reference terminals on the AMEL 2059 Potentiostat. The Potentiostat was operated at +0.455V with the Working terminal connected to the sample and ground. The output of the potentiostat was filtered by a Stanford Research Systems Dual Channel low-pass filter. The potentiostat output was fed into both input channels of the low-pass filter; each channel cutoff frequency was adjusted for each of the signal frequencies of interest: channel 1 had a cutoff frequency of 6Hz and was used to filter the fundamental 5Hz signal, while channel 2 had a cutoff frequency of 12 Hz and was

used to filter the  $2f$  (plastic) signal occurring at 10Hz. Each of the low-pass filter outputs, one at 5Hz and one at 10Hz, was sent to the input of a Stanford Research Systems SR830 Lock-in amplifier where both the phase and magnitude of the EFS signal could be obtained. The internal oscillator of the 5 Hz lock-in was used as the system's trigger, producing a 1V sine wave employed to drive the KEPCO op-amp and subsequently the linear actuator, as well as providing the reference signal for the 10Hz lock-in that was operated in  $2f$  mode.

Analog outputs from the lock-in amplifiers, as well as the 5Hz reference signal, were sent to a BNC-to-ribbon cable box, and then to a Computer Boards PCI-DAS 1602/16 16-bit, 16 channel A/D residing in a desktop computer. Data from the A/D could be collected and directly imported into an Excel spreadsheet for further analysis and plotting using software compatible with the Computer Boards A/D converter (Computer Boards DAS Wizard software). The entire EFS bench top system is depicted schematically in Figure 4.

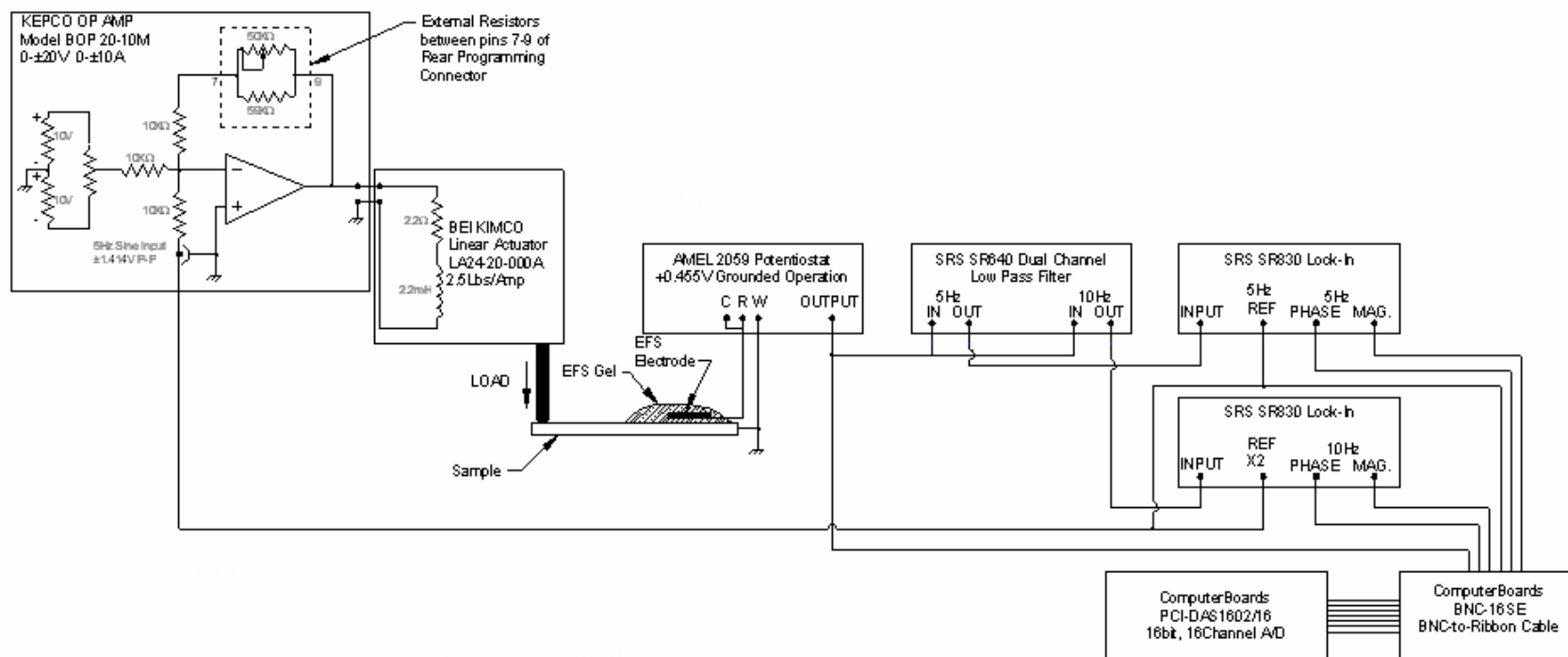


Figure 4. EFS Bench Top Block Diagram

## 2.4 EFS SIGNAL

As mentioned previously, the application of a sinusoidal load to the sample produces a pure sinusoidal EFS signal. While this signal can have higher harmonic components due to cracks, the signal is a simple waveform that can be easily filtered by conventional analog electronics. This avoids the rapid collection of thousands of noisy data points that must be digitally filtered and manipulated by software.

Raw EFS signal output from the potentiostat is in the micro amp range and contains a large amount of high frequency noise. In fact, typical potentiostat outputs are shown in Figure 5. The blue trace is the unfiltered EFS signal from the potentiostat, composed of

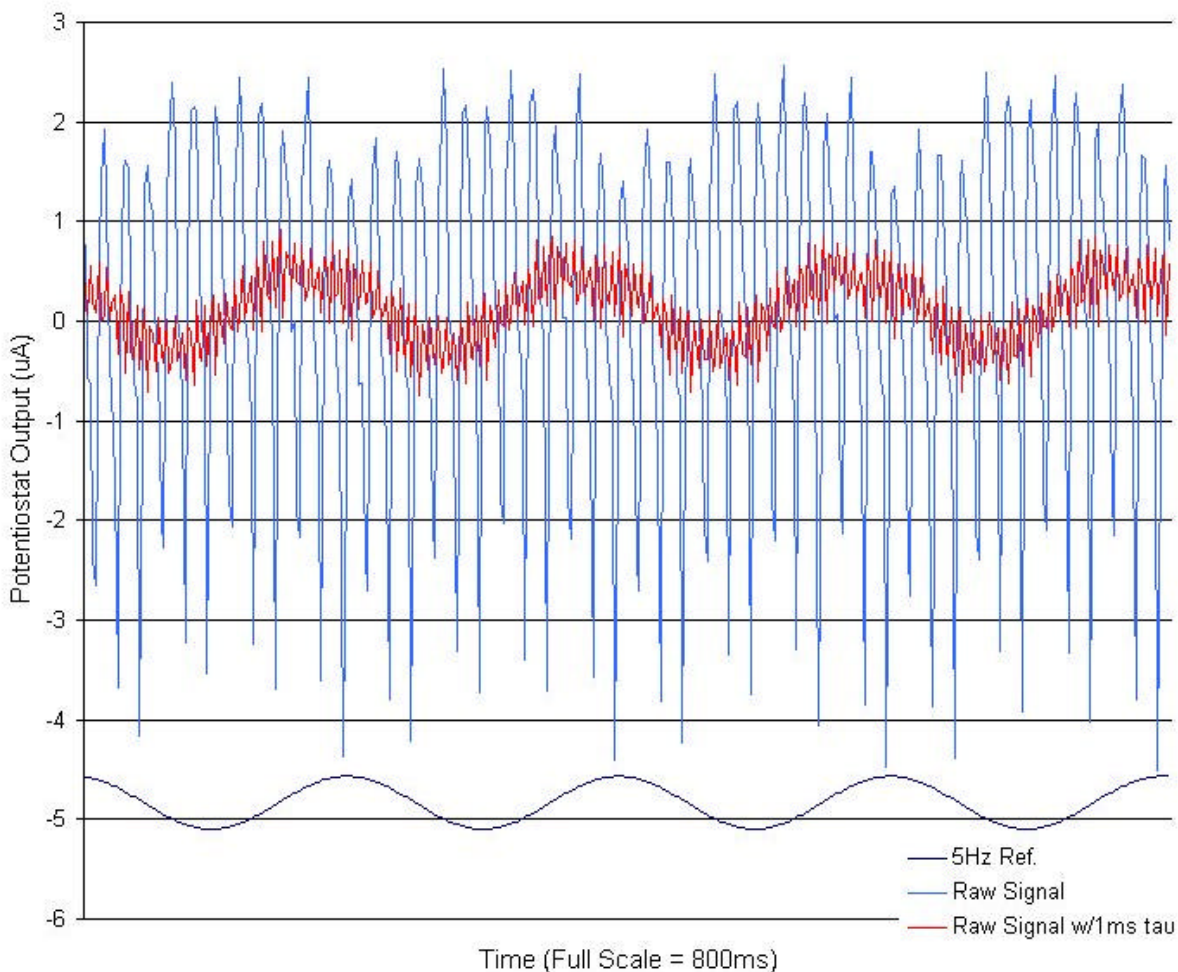


Figure 5. Potentiostat Output

primarily a 60Hz component and a small 120Hz component modulated at 5Hz – the modulation frequency of the applied load. In this situation, the 5Hz EFS signal is barely discernable from the noise, and exhibits a signal-to-noise ratio of approximately 1. Switching on the potentiostat's 1KHz low pass filter, which also includes a 60Hz notch filter, dramatically reduces the amount of 60Hz flicker, and improves the Signal-to-Noise



Ratio (S/N) to approximately 6. However, the 120Hz flicker and shot noise remain, even after selecting the potentiostat's output filter. While the shot noise could be reduced by integrating the signal longer (increasing the system's time constant), the 120Hz flicker cannot be significantly reduced by collecting more data. Therefore, digitally collecting this data, even over long periods of time, could somewhat reduce the line frequency and its harmonics noise contribution, but it could never eliminate it. Analog signal processing employing active filters, on the other hand, can dramatically reduce both the line frequency-generated flicker noise as well as the shot noise, dramatically improving the S/N over digital signal processing. This is important if this technique is to be used in the field because improving the S/N relates to the amount of time required to perform an analysis (the higher the S/N, the shorter the required integration time).

To ensure that we were indeed viewing actual EFS signals, rather than noise or coupling of the reference signal into the EFS electronics, data was collected in several different modes. This is depicted in Figure 6. With the Potentiostat Signal lead grounded through a 200 $\Omega$  resistor (blue trace), a small amount of signal is being detected by the potentiostat. Lowering the impedance to ground would have reduced or eliminated this, showing that there appears to be no induced signal through the electrode while in the EFS gel and in contact with the sample. The violet trace is the signal generated when the potentiostat signal lead is uncoupled from the gel and left floating in the air. This signal is probably a coupling of the induction coil driving the load actuator to the unshielded signal wire that is in close proximity. The green trace represents the signal generated when the entire system is configured to collect data, except the potentiostat's voltage is turned off. This is the background pick up of the EFS signal wire in the gel, again probably being influenced by the induction coil's radiation.

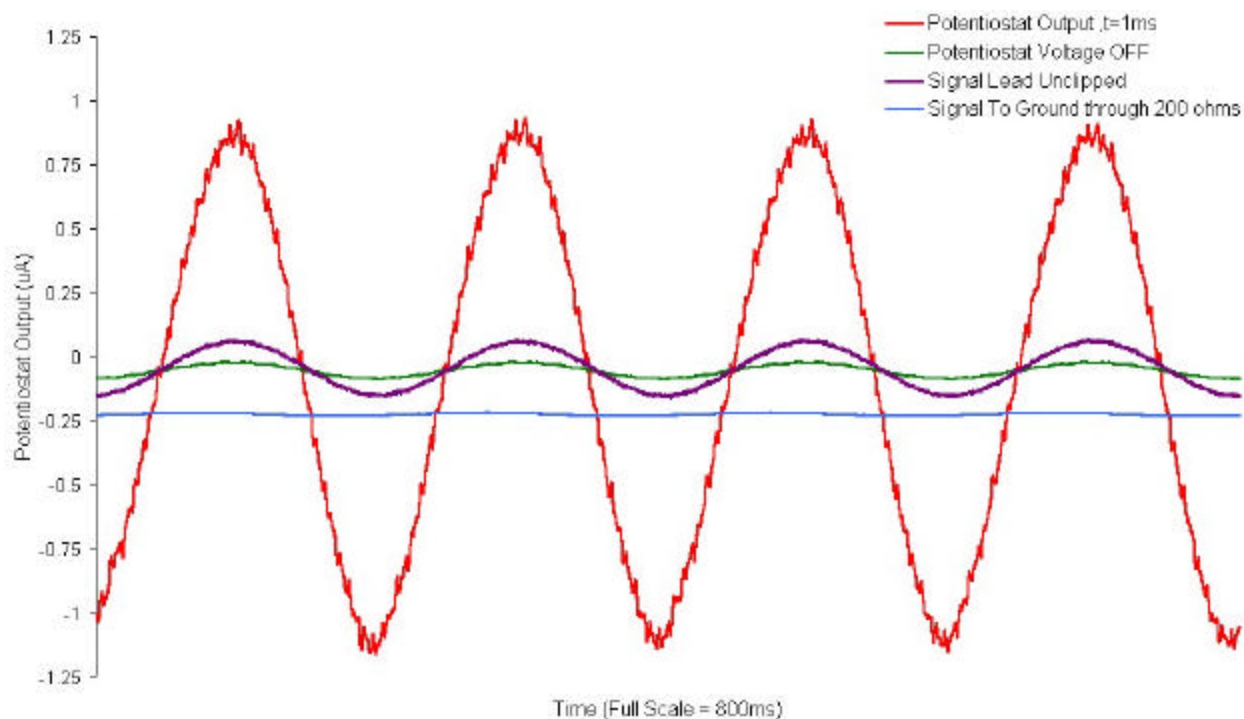


Figure 6. EFS Noise



The single frequency, 5Hz sinusoidal signal is indicative of an unstressed sample. However, when the sample begins to show signs of fatigue and develop cracks, the simple sinusoidal develops a higher frequency component at twice the reference signal. This is demonstrated in Figure 7 in which a 316 stainless steel sample was stressed for several hours, during which time the black 10Hz trace developed. The appearance of higher frequencies on the black 10Hz trace, such as the asymmetry on the leading edge of the sine wave and the bump on the trailing edge, are indications of the development of small cracks on the sample. Prior to this time, both the 5Hz and 10Hz signals appeared to be pure sine waves. Also, after this observation, the sample's surface was abraded and cleaned with fiberglass "Scotch-brite." After this cleaning, the 10Hz signal (side lobe on the descending edge of the 5Hz signal in the black trace) disappeared, apparently due to the removal of the micro cracks developed during the previous stress cycles. This also points to the validity of the "blending" process used to remove small visible cracks in the surface of turbine engine blades.

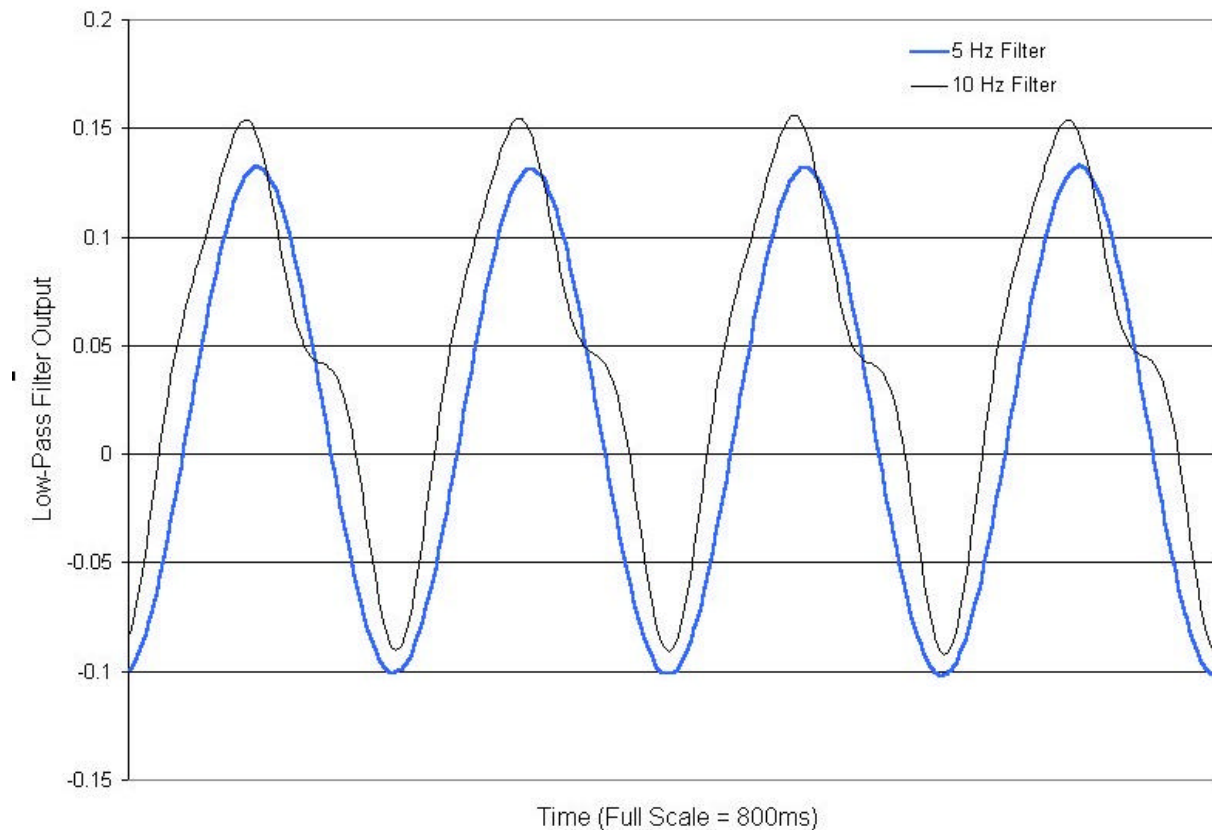


Figure 7. 5Hz and 10Hz Filtered EFS Signals

### 3.0 Ultrasonic Inspection

A portable, battery operated, Staveley Sonic 1200 HR ultrasonic electronics unit was coupled to the ultrasonic transducer (UT) probes to provide the pulsed signal to the transducer, collect the reflected pulses, and analyze and present the data. Two different types of UT probes were constructed: a shear wave (delay line) and a surface wave.

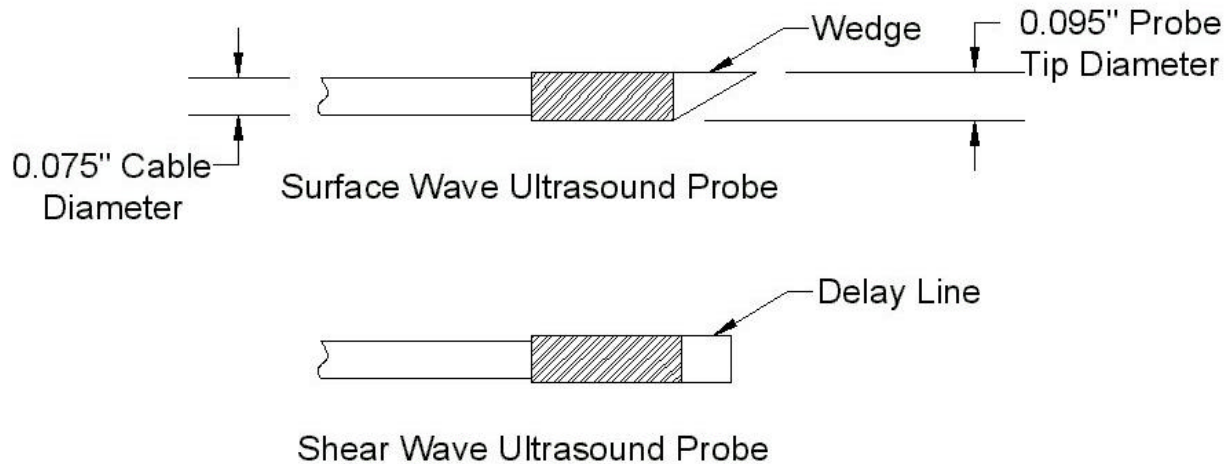


Figure 8. Ultrasound Probes

The delay line probe was used for checking the thickness of sample material, and had a thickness measurement range of 0.25 - 4.5mm. The transducer has an operating frequency of 10 MHz with a crystal diameter of 2.0mm. The tip of the probe measured 2.4mm diameter X 7.6mm long, and was made as small as reasonably possible in order to be able to transverse the 3mm working channel within the borescope, yet retain enough transducer area to produce signals with reasonable S/N.

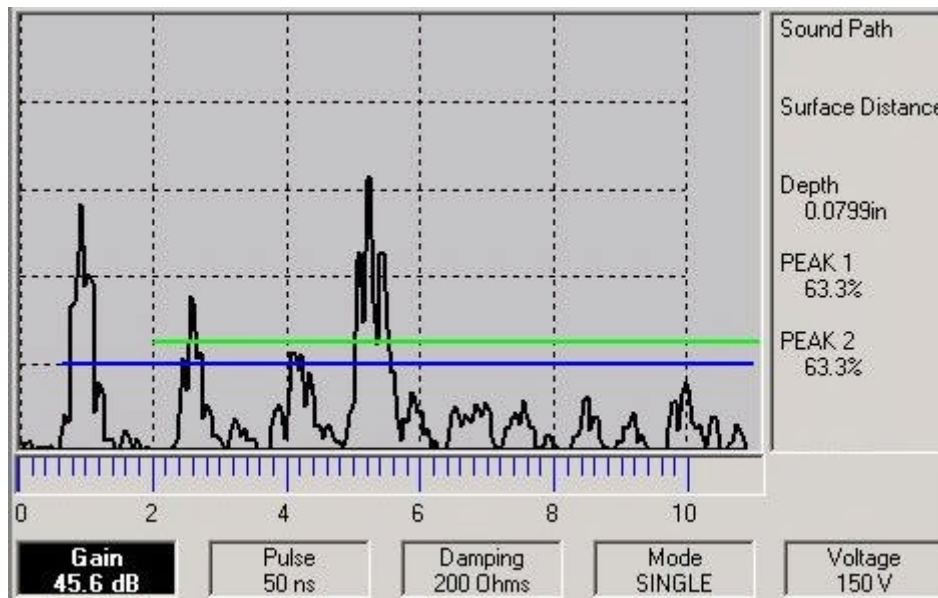


Figure 9. Delay Line Ultrasonic Display of 0.080" Thick Test Plate

The surface wave probe retained many of the characteristics of the delay line, both dimensionally and in operating frequency. The angled Lucite wedge at the front of the transducer provided more controllable surface contact than the delay line, making it easier to use for the operator. Also, the surface wave system permitted the detection of surface-breaking defects such as voids or cracks.

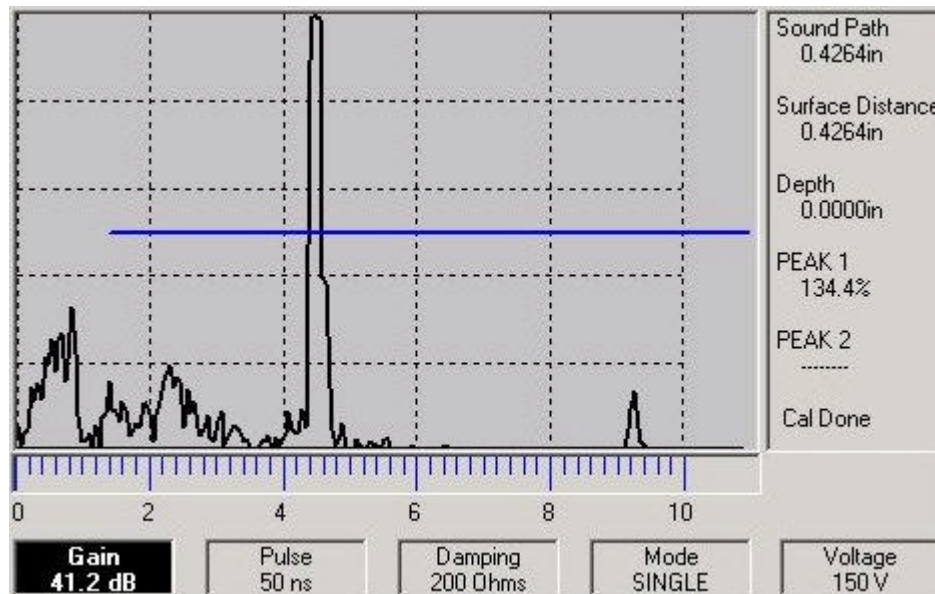


Figure 10. Surface Wave Ultrasonic Signal of Distant Crack  
(Crack is 0.43" From Sensor)

## 4.0 Eddy Current Inspection

A portable, battery operated, Staveley Nortec 2000S electronics unit was used for collecting and processing the eddy current probe data. First attempts at relative probes proved to be too sensitive to lift-off from the sample, and difficult to reduce in size to the required dimensions for passing through the working channel. We finalized on a miniature pencil probe with an absolute wound coil for the detection of surface breaking defects. The coil operated at a frequency of 1 MHz and had an outside diameter of 2.5mm. The absolute coil is unshielded, so that the sides of the probe can be used for scanning without concern for the probe's axial position with respect to the sample.

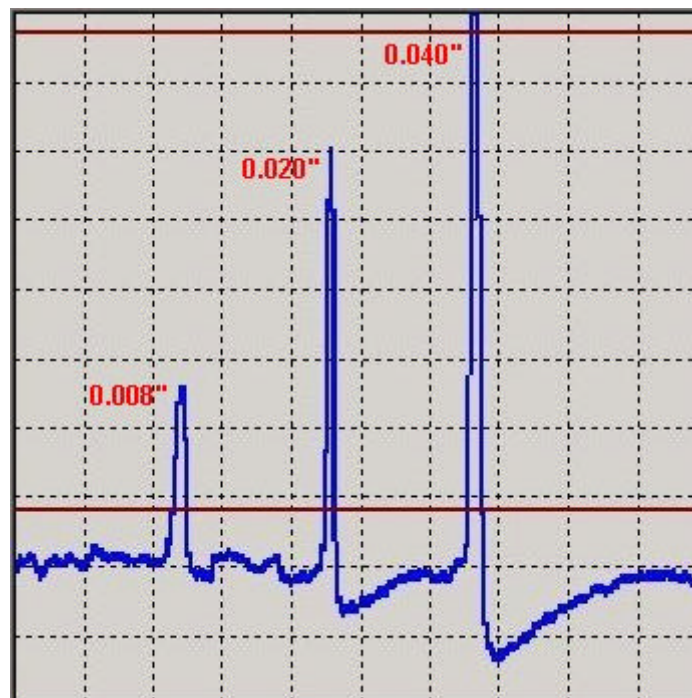


Figure 11. Absolute Eddy Current Signals from 0.005" Wide Cracks of Various Depths

## 5.0 Borescope Delivery System

Current borescope technology is unsuitable for fully interrogating components within an aircraft engine without disassembling the engine. The main focus of this investigation was to improve upon existing technology to produce a borescope engine inspection system that could:

- ❑ visually inspect the interior of an engine
- ❑ deliver ultrasonic probes within the engine
- ❑ deliver eddy current probes within the engine
- ❑ deliver EFS within an engine
- ❑ articulate 90° around a hemisphere at the distal end of the borescope
- ❑ provide an intuitive operator interface to articulation of the borescope
- ❑ maintain a borescope outer diameter of no more than 6mm

While working with the various probes configured for the borescope, it became apparent that several changes needed to be made to the design of the scope. Most apparent was the need for a different articulation mechanism than the traditional “two knob” system. The need arose because of the scanning requirements of the probes, particularly the eddy current probe. This probe requires that it be scanned over a crack in order to detect it. Scanning with the two-knob articulation mechanism required an extremely skilled operator and/or two hands on the scope handle/knobs. The operator would, therefore, need to release the scope shaft in order to operate the borescope’s articulation mechanism. This was unsatisfactory because both the eddy current and the ultrasonic probes are sensitive to lift off of the probe tip from the sample. We abandoned the original articulation design and modified an intuitive articulation mechanism that we developed for medical applications.

The current borescope design expands the scope’s ability to articulate, from the original 2-way articulation, where the distal tip had a range of  $\pm 70^\circ$  in only one plane, to Allway™ articulation whereby the scope’s tip can be pointed in any direction within a 90 degree hemisphere. This required the use of two sets of push/pull wires to accomplish articulation, but the typical two-knob articulation system was too cumbersome and difficult to use. The counterintuitive nature of the two-knob articulation mechanism was overcome by the implementation of a mechanical joystick. The joystick’s movement is intuitive, and directly relates to the direction of movement of the distal end of the borescope. The joystick can be operated with only one hand, thereby freeing the other hand to manipulate or support the scope shaft, or move probes and tools through the working channel. And, unlike an electronic servomotor driven joystick, a mechanical joystick is: more robust, simple, lighter, and it provides direct tactile feedback to the operator of any resistance that the scope’s tip is experiencing. Therefore, the operator is much less likely to overshoot the articulation mechanism, which could result in damage to the item being inspected, and damage to the borescope articulation mechanism and/or vertebrae.

Moving to the mechanical joystick, because of its intuitive nature and tactile feedback, also created unexpected problems with the way in which the original borescope was designed. There is a limited range of comfortable travel for a typical operator's thumb of approximately  $\pm 30^\circ$ . However, the borescope's end tip must articulate  $90^\circ$  in all directions. Since there is a minimum amount of torque required to articulate the scope, and a maximum amount of force a typical operator can comfortably exert on the joystick, a reexamination of torque, forces, gear ratios, and material selection had to be undertaken in order to make the joystick not only operable, but also comfortable to operate.

In order to reduce the amount of force required to articulate the borescope, several changes were made to the construction of the scope's insertion tube. The outer tungsten braid wire diameter was reduced slightly in order to minimize its stiffness while retaining its mechanical wear characteristics in protecting the scope from accidental damage. Along with this reduction the braid was manufactured on a smaller core than the shaft assembly. This forced the braid to be compressed over the vertebrae section thus creating a spring like characteristic that aids the vertebrae while articulating. The light guide were changed from 0.5mm diameter plastic fiber to bundles of 30 $\mu$ m diameter glass fibers, again to improve flexibility and cut down on the amount of force required to bend the end of the scope. One of the biggest challenges, and largest contributors to the scope's stiffness, was the working channel material. This channel must be able to smoothly and easily pass the various probes used to interrogate the sample, while at the same time be flexible and not kink when bent. We finalized on a thin-wall flexible PVC laminate in which a monocoil (spring) was embedded between two layers of elastomer. This provided the hoop strength to the channel material that prevented its collapse while bending, yet gave it enough flexibility so as not to add substantially to the stiffness of the shaft.

Yet another change for the final borescope design was the modification of the articulation vertebrae. The original vertebrae was designed for two-way articulation in a single plane of operation. While we have a 8mm diameter Allway™ vertebrae constructed of plastic links, the diameter of this vertebrae was too large for the current application, and it could not be scaled down in size to meet the 6mm maximum requirement for engine inspection. A new 6mm vertebrae was designed, with extremely thin walls, capable of articulating within a  $90^\circ$  hemisphere, and possessing a bend radius of 25mm. These changes were necessary in order to reduce the bending radius of the articulation section, which is critical in accessing tight spaces within an engine and for proper placement of the probes.



Figure 12. Articulation Link Pair.

The final vertebrae links were manufactured using EDM and grinding processes. This permitted the links to be manufactured from stainless steel, allowing wall thickness as low as 0.1mm, yielding more space for the working channel and other borescope internal components. This increase in interior area within the vertebrae also helped reduce the stiffness of the distal end of the shaft, further reducing the force required to articulate the shaft.

The above changes to the shaft components permitted the joystick mechanism to overcome the force and torque requirements needed to properly articulate the distal end of the scope. Additionally, these changes allowed the shaft length to increase, the bend radius to decrease, and sufficient space to permit the ultrasonic, eddy current, and EFS probes to be delivered through the borescope to a remote location.

## Borescope Specifications

### Mechanical Properties:

|                                 |                                |
|---------------------------------|--------------------------------|
| Outer Diameter                  | 6mm                            |
| Working Length                  | 1.5m                           |
| Working Channel Inside Diameter | 3mm                            |
| Articulation                    | 90° AllWay™ Articulation       |
| Minimum Bend Radius             | 25mm                           |
| Shaft Covering                  | Braided Tungsten over Urethane |
| Operating Temperature           | 0-54°C                         |
| Handle                          | Custom SLA                     |
| Storage Case                    | Gray Pelican                   |

### Optical Properties:

|                     |   |
|---------------------|---|
| Dept of Field       | 5-50mm  |
| Field of View       | 50°   |
| Resolution          | 2 lp/mm at 5mm  |
| Image Bundle        | 0.4mm diameter Quartz<br>6,000 pixels   |
| Video Direct Imager | 1/3" Color CCD<br>410,000 pixels<br>768 (H) x 494 (V) Video Resolution  |
| Light Guide         | Detachable Glass, ACMI Connector  |
| Light Source        | MS-48 Portable/Rechargeable<br>12V, 2A Metal Halide<br>5460 Color Temperature<br>Rechargeable Li-Ion Battery / 115VAC |



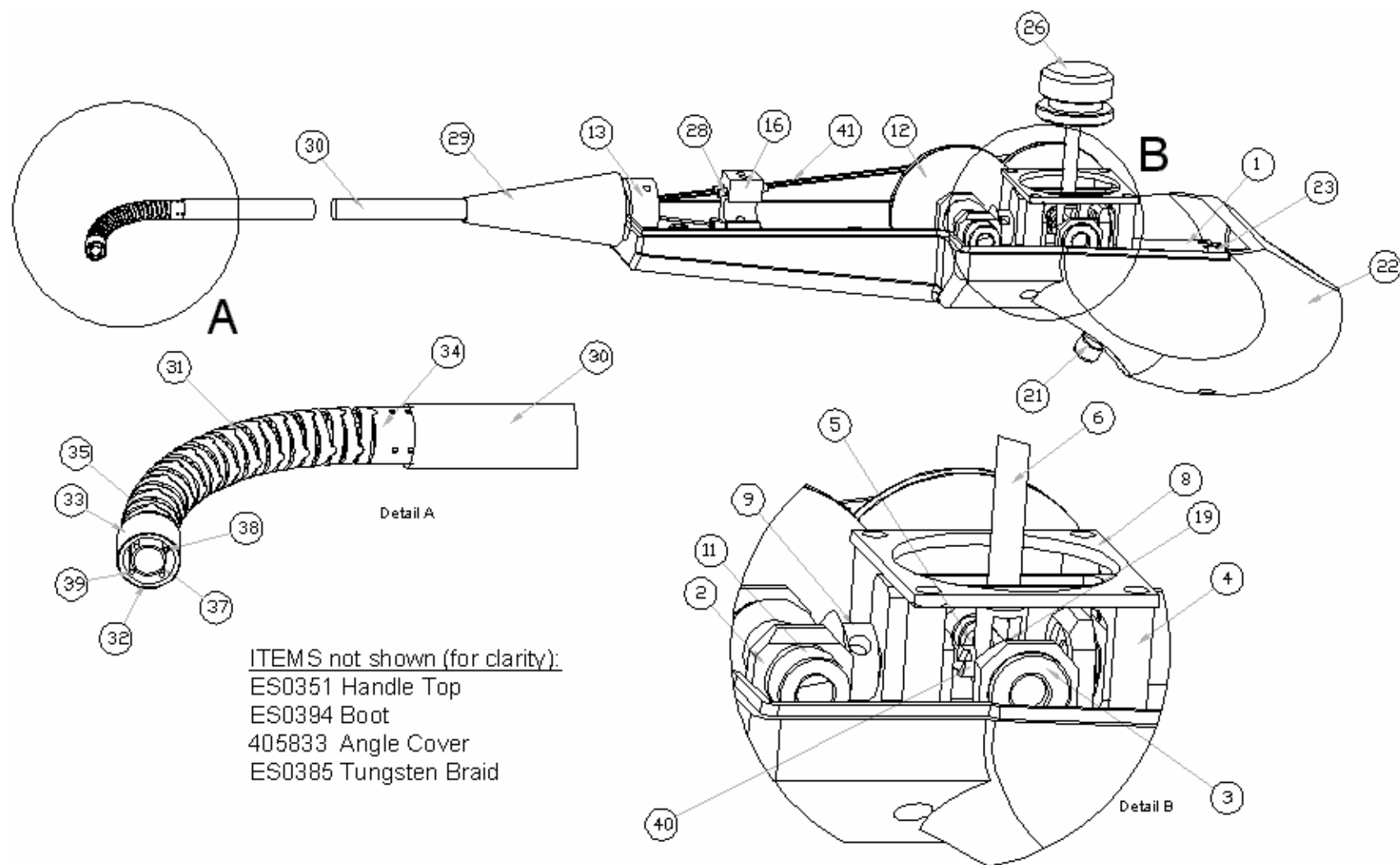


Figure 13. Borescope Assembly

## Borescope Assembly Bill of Material

| Item # | Part # | Description        |
|--------|--------|--------------------|
| 1      | ES0347 | BASE PLATE         |
| 2      | ES0337 | BEARING BLOCK      |
| 3      | ES0310 | BEARING            |
| 4      | ES0392 | STANDOFF           |
| 5      | ES0335 | PULLY ARM          |
| 6      | ES0336 | ARM COUPLER        |
| 7      | ES0338 | ARC GUIDE          |
| 8      | ES0346 | STOP PLATE         |
| 9      | ES0339 | GEAR MODIFIED      |
| 10     | ES0340 | SHAFT LONG         |
| 11     | ES0302 | SHAFT COLLAR       |
| 12     | ES0300 | DRUM               |
| 13     | ES0124 | SHAFT COUPLER      |
| 14     | ES0027 | CAMERA             |
| 15     | ES0107 | CAMERA BLOCK       |
| 16     | ES0348 | SPRING GUIDE BLOCK |
| 17     | ES0367 | LUER FITTING MOD   |
| 18     | ES0341 | SHAFT SHORT        |
| 19     | ES0390 | WASHER TEFLON      |
| 20     | ES0344 | SHAFT SPACER       |
| 21     | ES0397 | ACMI CONNECTOR     |
| 22     | ES0350 | HANDLE BOTTOM      |

|    |        |                     |
|----|--------|---------------------|
| 23 | ES0393 | SPACER              |
| 24 | ES0387 | GROMMET             |
| 25 | ES0343 | ACMI MOUNT          |
| 26 | ES0349 | JOYSTICK CAP        |
| 27 | ES0342 | SHAFT MID           |
| 28 | ES0398 | SPRING GUIDE STOP   |
| 29 | 405787 | STRAIN RELIEF       |
| 30 | ES0404 | MASTER SHEATHING    |
| 31 | 004871 | VERTEBRAE LINK      |
| 32 | ES0361 | HEAD DISTAL         |
| 33 | ES0360 | SLEEVE HEAD         |
| 34 | ES0362 | SPRING GUIDE COLLAR |
| 35 | ES0401 | VERTIBREA LINK MOD  |
| 36 | ES0372 | SPRING GUIDE SLEEVE |
| 37 | ES0384 | WORKING CHANNEL     |
| 38 | ES0395 | QUARTZ IMAGE GUIDE  |
| 39 | 012045 | LIGHT GUIDE FIBER   |
| 40 | ES0391 | COUPLER SCREW       |
| 41 | 409048 | CONTROL WIRE        |
| 42 | ES0351 | HANDLE TOP          |
| 43 | ES0394 | BOOT                |
| 44 | 405833 | ANGLE COVER         |
| 45 | ES0385 | BRAID TUNGSTEN      |

## 6.0 Conclusions

Improvements to current borescope design, including a more intuitive articulation mechanism and the development of a 6mm diameter borescope with a 3mm diameter working channel, permit the delivery of visual, ultrasonic, eddy current, and EFS probes to internal components of aircraft engine. Current technologies that produce sufficient force to result in EFS signals, however, are too large to be delivered within the 6mm diameter access to the engine. Nonetheless, the ability to visually inspect engine components, and then verify the presence or absence of cracks with eddy current or ultrasonic probes, is a valuable tool for the nondestructive testing of aircraft fatigue critical locations.

Future work should incorporate all system components (borescope, light source, video display, computer, eddy current and ultrasonic electronics, and EFS) into a single, portable instrument. An effort is also needed to produce user-friendly software to operate the instrumentation, and to integrate the data from the various sensors into a single database. More ergonomic design work is also necessary for the joystick handle.

Also needed for EFS to function within an on-wing aircraft engine is a mechanism to apply the necessary load for the production of an EFS signal. Currently, the technology is not available to apply the necessary load within the tight confines of an engine. In future engine designs, this mechanism, or an access port for the mechanism, could be designed into the engine.

## Appendix A: Borescope Detail Drawing List

| FILE NAME                            | SIZE  | FILE TYPE              |
|--------------------------------------|-------|------------------------|
| 2100r0 (NECP-1010-R1) EDDY PROBE.PDF | 19KB  | Adobe Acrobat Document |
| ES0020 MONOCOIL.DWG                  | 61KB  | AutoCAD Drawing        |
| ES0021 SHEATHING.DWG                 | 55KB  | AutoCAD Drawing        |
| ES0024 SPRING GUIDE.DWG              | 55KB  | AutoCAD Drawing        |
| ES0027 CAMERA.DWG                    | 55KB  | AutoCAD Drawing        |
| ES0027 CAMERA.SLDPRT                 | 53KB  | SLDPRT File            |
| ES0063 COUPLER HOUSING.DWG           | 60KB  | AutoCAD Drawing        |
| ES0064 LENS BARREL.DWG               | 49KB  | AutoCAD Drawing        |
| ES0070 NUT.DWG                       | 44KB  | AutoCAD Drawing        |
| ES0079 LENS.DWG                      | 44KB  | AutoCAD Drawing        |
| ES0080 LENS ASSEMBLY.DWG             | 41KB  | AutoCAD Drawing        |
| ES0083 LUER FITTING.DWG              | 44KB  | AutoCAD Drawing        |
| ES0107 CAMERA BASE.DWG               | 51KB  | AutoCAD Drawing        |
| ES0107 CAMERA BLOCK.SLDPRT           | 92KB  | SLDPRT File            |
| ES0124 SHAFT COUPLER.DWG             | 59KB  | AutoCAD Drawing        |
| ES0124 SHAFT COUPLER.SLDPRT          | 103KB | SLDPRT File            |
| ES0300 DRUM.DWG                      | 60KB  | AutoCAD Drawing        |
| ES0300 DRUM.SLDPRT                   | 118KB | SLDPRT File            |
| ES0301 GEAR.DWG                      | 58KB  | AutoCAD Drawing        |
| ES0302 COLLAR.DWG                    | 56KB  | AutoCAD Drawing        |
| ES0302 SHAFT COLLAR.SLDPRT           | 202KB | SLDPRT File            |
| ES0310 BEARING.DWG                   | 59KB  | AutoCAD Drawing        |
| ES0310 BEARING.SLDPRT                | 116KB | SLDPRT File            |
| ES0335 PULLY ARM.SLDDRW              | 328KB | SLDDRW File            |
| ES0335 PULLY ARM.SLDPRT              | 123KB | SLDPRT File            |
| ES0336 ARM COUPLER.SLDDRW            | 332KB | SLDDRW File            |
| ES0336 ARM COUPLER.SLDPRT            | 167KB | SLDPRT File            |
| ES0337 BEARING BLOCK.SLDDRW          | 285KB | SLDDRW File            |
| ES0337 BEARING BLOCK.SLDPRT          | 119KB | SLDPRT File            |
| ES0338 ARC GUIDE.SLDDRW              | 325KB | SLDDRW File            |
| ES0338 ARC GUIDE.SLDPRT              | 205KB | SLDPRT File            |
| ES0339 GEAR MODIFIED.SLDDRW          | 292KB | SLDDRW File            |
| ES0339 GEAR MODIFIED.SLDPRT          | 122KB | SLDPRT File            |
| ES0340 SHAFT LONG.SLDDRW             | 268KB | SLDDRW File            |
| ES0340 SHAFT LONG.SLDPRT             | 94KB  | SLDPRT File            |
| ES0341 SHAFT SHORT.SLDDRW            | 293KB | SLDDRW File            |
| ES0341 SHAFT SHORT.SLDPRT            | 88KB  | SLDPRT File            |
| ES0342 SHAFT MID.SLDDRW              | 294KB | SLDDRW File            |
| ES0342 SHAFT MID.SLDPRT              | 76KB  | SLDPRT File            |
| ES0343 ACMI MOUNT.SLDDRW             | 324KB | SLDDRW File            |

**Appendix A: Borescope Detail Drawing List**  
continued

| FILE NAME                         | SIZE    | FILE TYPE       |
|-----------------------------------|---------|-----------------|
| ES0343 ACMI MOUNT.SLDPRT          | 104KB   | SLDPRT File     |
| ES0344 SHAFT SPACER.SLDDRW        | 286KB   | SLDDRW File     |
| ES0344 SHAFT SPACER.SLDPRT        | 82KB    | SLDPRT File     |
| ES0346 STOP PLATE.SLDDRW          | 333KB   | SLDDRW File     |
| ES0346 STOP PLATE.SLDPRT          | 110KB   | SLDPRT File     |
| ES0347 BASE PLATE HOLE DIM.SLDDRW | 633KB   | SLDDRW File     |
| ES0347 BASE PLATE.SLDDRW          | 597KB   | SLDDRW File     |
| ES0347 BASE PLATE.SLDPRT          | 452KB   | SLDPRT File     |
| ES0348 SPRING GUIDE BLOCK.SLDDRW  | 454KB   | SLDDRW File     |
| ES0348 SPRING GUIDE BLOCK.SLDPRT  | 292KB   | SLDPRT File     |
| ES0349 JOYSTICK CAP.SLDDRW        | 325KB   | SLDDRW File     |
| ES0349 JOYSTICK CAP.SLDPRT        | 86KB    | SLDPRT File     |
| ES0350 HANDLE BOTTOM.SLDDRW       | 550KB   | SLDDRW File     |
| ES0350 HANDLE BOTTOM.SLDPRT       | 1,166KB | SLDPRT File     |
| ES0351 HANDLE TOP.SLDDRW          | 228KB   | SLDDRW File     |
| ES0351 HANDLE TOP.SLDPRT          | 744KB   | SLDPRT File     |
| ES0360 SLEEVE HEAD.SLDDRW         | 140KB   | SLDDRW File     |
| ES0360 SLEEVE HEAD.SLDPRT         | 73KB    | SLDPRT File     |
| ES0361 HEAD DISTAL.SLDDRW         | 299KB   | SLDDRW File     |
| ES0361 HEAD DISTAL.SLDPRT         | 196KB   | SLDPRT File     |
| ES0362 SPRING GUIDE COLLAR.SLDDRW | 352KB   | SLDDRW File     |
| ES0362 SPRING GUIDE COLLAR.SLDPRT | 219KB   | SLDPRT File     |
| ES0367 LUER FITTING MOD.SLDPRT    | 84KB    | SLDPRT File     |
| ES0368 MASTER SHEATHING.DWG       | 123KB   | AutoCAD Drawing |
| ES0368 MASTER SHEATHING.SLDPRT    | 55KB    | SLDPRT File     |
| ES0372 SPRING GUIDE SLEEVE.SLDDRW | 287KB   | SLDDRW File     |
| ES0372 SPRING GUIDE SLEEVE.SLDPRT | 68KB    | SLDPRT File     |
| ES0384 WORKING CHANNEL.SLDPRT     | 35KB    | SLDPRT File     |
| ES0385 BRAID.DWG                  | 85KB    | AutoCAD Drawing |
| ES0387 GROMMET.SLDDRW             | 132KB   | SLDDRW File     |
| ES0387 GROMMET.SLDPRT             | 85KB    | SLDPRT File     |
| ES0388 SPRING WASHER.SLDDRW       | 132KB   | SLDDRW File     |
| ES0390 WASHER TEFLON.SLDPRT       | 28KB    | SLDPRT File     |
| ES0391 COUPLER SCREW.SLDDRW       | 278KB   | SLDDRW File     |
| ES0391 COUPLER SCREW.SLDPRT       | 99KB    | SLDPRT File     |
| ES0391 WASHER TEFLON.SLDDRW       | 133KB   | SLDDRW File     |
| ES0392 STANDOFF.SLDDRW            | 269KB   | SLDDRW File     |
| ES0392 STANDOFF.SLDPRT            | 56KB    | SLDPRT File     |
| ES0393 SPACER.SLDDRW              | 266KB   | SLDDRW File     |

**Appendix A: Borescope Detail Drawing List**  
continued

| FILE NAME                                     | SIZE    | FILE TYPE       |
|---|---------|-----------------|
| ES0393 SPACER.SLDPRT                          | 59KB    | SLDPRT File     |
| ES0394 BOOT.SLDPRT                            | 326KB   | SLDPRT File     |
| ES0395 QUARTZ IMAGE GUIDE LENSED.DWG          | 57KB    | AutoCAD Drawing |
| ES0395 QUARTZ IMAGE GUIDE.SLDPRT              | 33KB    | SLDPRT File     |
| ES0396 SCOPE ASSEMBLY.SLDASM                  | 1,805KB | SLDASM File     |
| ES0396 SCOPE ASSEMBLY.SLDDRW                  | 827KB   | SLDDRW File     |
| ES0397 ACMI CONNECTOR.DWG                     | 70KB    | AutoCAD Drawing |
| ES0397 ACMI CONNECTOR.SLDPRT                  | 166KB   | SLDPRT File     |
| ES0398 SPRING GUIDE STOP.SLDDRW               | 275KB   | SLDDRW File     |
| ES0398 SPRING GUIDE STOP.SLDPRT               | 40KB    | SLDPRT File     |
| ES0399 HANDLE ASSEMBLY.SLDDRW                 | 115KB   | SLDDRW File     |
| ES0400 DISTAL ASSEMBLY.SLDASM                 | 595KB   | SLDASM File     |
| ES0401 VERTIBREA LINK MOD.SLDPRT              | 246KB   | SLDPRT File     |
| ES0402 QUARTZ BUNDLE HOLDER.SLDDRW            | 365KB   | SLDDRW File     |
| ES0402 QUARTZ BUNDLE HOLDER.SLDPRT            | 89KB    | SLDPRT File     |
| ES0403 COUPLER HOUSING.DWG                    | 66KB    | AutoCAD Drawing |
| ES0405 SHAFT SLEEVE.SLDDRW                    | 109KB   | SLDDRW File     |
| ES0405 SHAFT SLEEVE.SLDPRT                    | 36KB    | SLDPRT File     |
| ES0406 FERRULE FOR IMAGE BUNDLE.SLDDRW        | 130KB   | SLDDRW File     |
| ES0406 FERRULE FOR IMAGE BUNDLE.SLDPRT        | 34KB    | SLDPRT File     |
| ES0409 COUPLING DELIVERY SYSTEM.SLDDRW        | 115KB   | SLDDRW File     |
| ES0410 EFS WIRING HARNESS                     | 353KB   | SLDDRW File     |
| ES0411 BNC T                                  | 299KB   | SLDDRW File     |
| 004871 VERTEBRAE LINK.SLDPRT                  | 343KB   | SLDPRT File     |
| 004871 VERTIBREA LINK ASSEMBLY.SLDASM         | 174KB   | SLDASM File     |
| 004871 VERTEBRAE LINK REV 8.DWG               | 100KB   | AutoCAD Drawing |
| 012045 LIGHT GUIDE FIBER.SLDPRT               | 32KB    | SLDPRT File     |
| 405787 STRAIN RELIEF.DWG                      | 53KB    | AutoCAD Drawing |
| 405787 STRAIN RELIEF.SLDPRT                   | 85KB    | SLDPRT File     |
| 409048 CONTROL WIRE.SLDPRT                    | 34KB    | SLDPRT File     |
| CX227A UT DELAY PROBE.DWG                     | 18KB    | AutoCAD Drawing |
| CX228A UT SURFACE PROBE.DWG                   | 21KB    | AutoCAD Drawing |
|   |         |                 |
| ORIENTATION BLOCK.SLDPRT (for reference only) | 106KB   | SLDPRT File     |
| TEMPLATE.SLDDRW (for reference only)          | 227KB   | SLDDRW File     |

## Appendix B: EFS Electronics Settings

- AMEL 2059 Potentiostat
  - +0.455V Grounded Operation
  - Working Electrode and Sample connected to ground
  - Counter and Reference Electrode connected to EFS Electrode
  - Potential Current Potentiostat = 0.1
  - Backing Off = Off
  - IR Compression = Off
  - V(out) = Off
  - Function = Potentiostat (button in)
  - Polarity = + (button in)
- SR640 Dual Channel Low-Pass Filter
  - CHANNEL 1:
    - AC Coupled
    - 6 Hz
    - Gain (input) = 20dB
    - Gain (output) = 0dB
  - CHANNEL 2:
    - AC Coupled
    - 16 Hz
    - Gain (input) = 30dB
    - Gain (output) = 10dB
- SR803 Lock-In Amplifier #1 – 10 Hz Signal
  - $\tau = 10s$
  - Sensitivity = 50mV
  - Signal Input = A
  - Reserve = Normal
  - Filters = Line
  - CH1 Output = X
  - CH2 Output =  $\theta$
  - Harmonic = 2
  - Frequency Reference Input from Lock-In #2 @ 5Hz
- SR803 Lock-In Amplifier #2 – 5Hz
  - $\tau = 10s$
  - Sensitivity = 50mV
  - Signal Input = A
  - Reserve = Normal
  - Filters = Line
  - CH1 Output = X
  - CH2 Output =  $\theta$
  - Amplitude = 0.150V
  - Reference Frequency = 5.000Hz

- PCI-DAS 1602-16 16 Channel A/D
  - Input Voltage Range =  $\pm 10V$
  - Channel Assignments:
    - Ch1 – 5Hz Reference
    - Ch2 – Potentiostat Output
    - Ch3 – 5Hz Lock-In X
    - Ch4 – 5Hz Lock-In  $\theta$
    - Ch5 – 10Hz Lock-In X
    - Ch6 – 10Hz Lock-In  $\theta$
    - Ch7 – 5Hz Low-Pass Filter Output
    - Ch8 – 10Hz Low-Pass Filter Output
- KEPCO BOP 20-10M Op-Amp
  - Reference Input = 5Hz Sine Wave from 5Hz Lock-In Reference Output
  - External Resistor (Back Panel) =  $59K\Omega$  (fixed) in parallel with  $50K\Omega$  Pot.
  - Minimum Load Settings:
    - Force = 4 pounds
    - Output Current = 1.6A
    - Output Voltage = 3.52V
  - Maximum Load Settings:
    - Force = 15 pounds
    - Output Current = 6.0A
    - Output Voltage = 13.2V



### Appendix C: Eddy Current Probe Standard Programs

|             | Steel   | Aluminum |
|-------------|---------|----------|
| Frequency   | 1.0 MHz | 1.0 MHz  |
| H-Gain      | 69.1 dB | 62.8 dB  |
| V-Gain      | 69.1 dB | 82.8 dB  |
| Angle       | 240.3   | 249.1    |
| H-Position  | 50.0%   | 50.0%    |
| V-Position  | 30.0%   | 30.0%    |
| LP Filter   | 100     | 100      |
| HP Filter   | Off     | Off      |
| Sweep       | 1.000s  | 1.000s   |
| Cont Null   | 1.0 Hz  | 1.0 Hz   |
| Prove Driv  | Mid     | Mid      |
| Sweep Erase | On      | On       |
| Dot/Box     | Box     | Box      |
| Horn        | Off     | Off      |
| Capture     | 2.5 s   | 5.0 s    |
| Disp Ers    | Off     | Off      |
| Graticule   | On      | On       |
| Persist     | Off     | Off      |
| Alarm       | Sweep   | Sweep    |
| Alarm Dwell | 0       | 0        |
| Sweep       | Off     | Negative |
| Top         | 75.0%   | 72.0%    |
| Bottom      | 25.0%   | 3.0%     |

## Appendix D: Ultrasonic Probe Standard Programs

|                 | Surface Wave<br>Probe | Shear Wave<br>No Delay | Shear Wave<br>Delay |
|-----------------|-----------------------|------------------------|---------------------|
| <b>PULSER</b>   |                       |                        |                     |
| Pulser          | 50 ns                 | 50 ns                  | 50 ns               |
| Damping         | 200                   | 200                    | 200                 |
| Mode            | Single                | Single                 | Single              |
| Voltage         | 150 V                 | 150 V                  | 150 V               |
|                 |                       |                        |                     |
| <b>RECEIVER</b> |                       |                        |                     |
| Gain            | 41.2 dB               | 72.4 dB                | 52.6 dB             |
| Display         | Fullwave              | Fullwave               | Fullwave            |
| Frequency       | 10 MHz                | 10 MHz                 | 10 MHz              |
| Reject          | 0%                    | 0%                     | 0%                  |
| DB Diff         | 0 dB                  | 0 dB                   | 0 dB                |
|                 |                       |                        |                     |
| <b>GATE</b>     |                       |                        |                     |
| Gate 1          | +                     | +                      | +                   |
| Level           | 44%                   | 50%                    | 31%                 |
| Position        | 0.439 in              | 0.173 in               | 0.318 in            |
| Width           | 2.0 in                | 1.000 in               | 1.000 in            |
| Gate 2          | Off                   | +                      | +                   |
| Level           | 50%                   | 58%                    | 35%                 |
| Position        | 0.500 in              | 0.070 in               | 0.029 in            |
| Width           | 0.250 in              | 1.000 in               | 1.000 in            |
|                 |                       |                        |                     |
| <b>RANGE</b>    |                       |                        |                     |
| Range           | 1.000 in              | 1.000 in               | 0.250 in            |
| Delay           | 0.284 in              | 0.000 I                | 0.262 in            |
| Vel             | 0.1260                | 0.2310                 | 0.2310              |
| Rep Rate        | 150 Hz                | 2000 Hz                | 2000 Hz             |
| DAC             | Off                   | Off                    | Off                 |

**Appendix D: Ultrasonic Probe Standard Programs**  
continued

|                  | Surface Wave<br>Probe | Shear Wave<br>No Delay | Shear Wave<br>Delay |
|------------------|-----------------------|------------------------|---------------------|
| <b>SPCL</b>      |                       |                        |                     |
| Units            | in                    | in                     | in                  |
| +dB Val          | 6.0 dB                | 6.0 dB                 | 6.0 dB              |
| Peakhold         | Off                   | Off                    | Off                 |
|                  |                       |                        |                     |
| <b>THICKNESS</b> |                       |                        |                     |
| T-Gauge          | IP-1 <sup>st</sup>    | Auto E-E               | Auto E-E            |
| Trigger          | Edge                  | Edge                   | Edge                |
| Offset           | 6.475 us              | 0.000 us               | 0.000 us            |
| T-Vel            | 0.2432                | 0.2310                 | 0.2310              |
| Trip             | Off                   | Off                    | Off                 |
| Angle            | 90.0                  | 90.0                   | 0                   |
| Thick            | 0.0973                | 0.0996 in              | 0.0996 in           |
| O-Diam           | Off                   | Off                    | Off                 |